Chapter 11

Ultrafast lasers

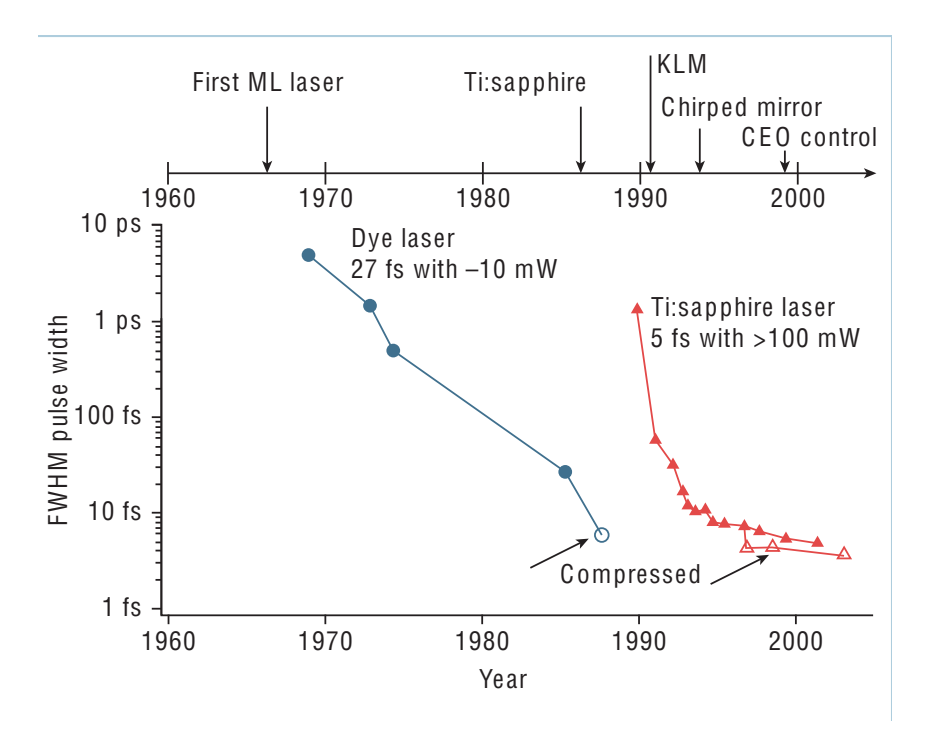


Figure 11.1: Improvements in ultrashort pulse generation since the first demonstration of a laser in 1960. Until the end of the 1980s, ultrashort pulse generation was dominated by dye lasers, and pulses as short as 27 fs with an average power of ≈10 mW were achieved at a centre wavelength of 630 nm. External pulse compression ultimately resulted in pulses as short as 6 fs a world record result by C. V. Shanks group that was not surpassed for about 10 years. This situation changed with the discovery of the Ti:sapphire laser. Today, pulses with only two optical cycles at FWHM (full-width half-maximum) at a centre wavelength of 800 nm have been generated with Ti:sapphire lasers with more than 100 mW average output power. External compression resulted in pulses as short as 3.8 fs. The filled symbols indicate results directly achieved from a laser; open symbols indicate results achieved with additional external pulse compression. ¹

 $^{^1}$ Source: Recent developments in compact ultrafast lasers, Ursula Keller, insight review articles, NATURE, VOL 424, 14 AUGUST 2003

11.1 Introduction to Optical Pulses²

It is quite easy to produce "gedanken" light pulses. Let us start with a monochromatic plane wave, previously defined as (Fig.11.2)

$$E_y = Re\left(E_0 e^{i\omega_0 t}\right) \tag{11.1.1}$$

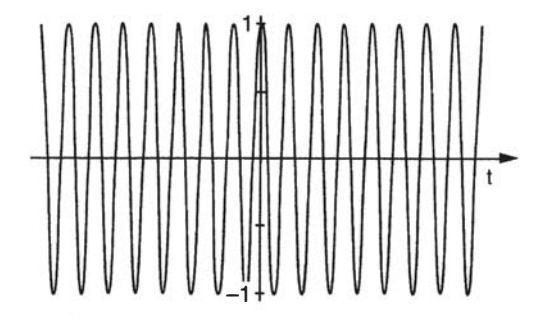


Figure 11.2: Schematic diagram of a heterodyne detector using a photomultiplier.

The time representation of the field is an unlimited cosine function. Constructing a light pulse implies multiplying (11.1.1) by a bell-shaped function. To simplify further calculation, we choose to multiply by a Gaussian function. A Gaussian pulse can be written

$$E_y = Re\left(E_0 e^{-\Gamma t^2 + i\omega_0 t}\right) \tag{11.1.2}$$

and its time evolution is shown in Fig. 11.3.

 Γ is the shape factor of the Gaussian envelope; it is proportional to the inverse of the squared duration to, i.e. $\Gamma \propto t_0^{-2}$.

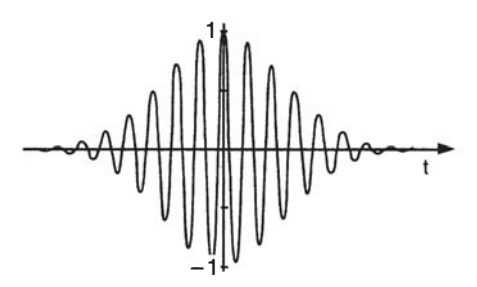


Figure 11.3: Schematic diagram of a heterodyne detector using a photomultiplier.

Let us now turn to the spectral content of a light pulse. This can be obtained by calculating the modules of the Fourier transform of the time evolution function of the pulse. As said earlier, a plane wave oscillates with the unique angular frequency ω_0 and its Fourier transform is a Dirac distribution $\delta(\omega_0)$ (Fig. (11.4)).

The Fourier transform of a Gaussian pulse is also a Gaussian function (Fig.11.5). Therefore the frequency content of a light pulse is larger than the unique frequency of a plane wave. The mathematical expression for the spectrum is given in Fig. 11.5 and the width of the spectrum is proportional to Γ .

 $^{^2}$ Chapter 2 (Page 28 - 32) - Femtosecond laser pulses : principles and experiments -Rulliere, Claude - New York : Springer, 2005

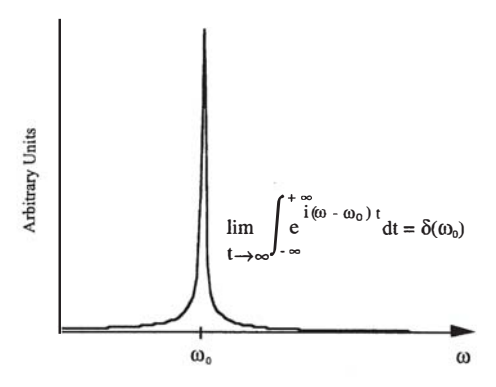


Figure 11.4: Numerical Fourier transform of the truncated cosine function shown in Fig. (11.2). As the width of the cosine function grows larger and larger $(t_0 \to \infty)$, the Fourier transform tends toward a Dirac distribution $\delta(\omega_0)$ with zero width

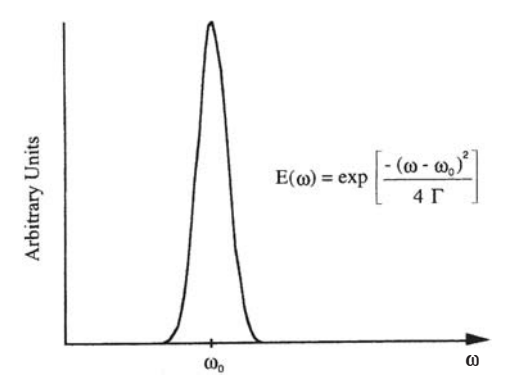


Figure 11.5: Numerical Fourier transform of the truncated cosine function shown in Fig. (11.2). As the width of the cosine function grows larger and larger $(t_0 \to \infty)$, the Fourier transform tends toward a Dirac distribution $\delta(\omega_0)$ with zero width

Relationship Between Duration and Spectral Width

We have just empirically observed that the spectral width and the duration of a pulse are related quantities. What is the exact relationship? We start from the general time and frequency Fourier transforms of a pulse:

$$\epsilon(t) = \frac{1}{2\pi} \int_{-\infty}^{\infty} E(\omega) e^{-i\omega t} d\omega, \qquad E(\omega) = \frac{1}{2\pi} \int_{-\infty}^{\infty} \epsilon(t) e^{i\omega t} dt$$
 (11.1.3)

When the duration and the spectral width oft he pulse are calculated using the standard statistical definitions

$$\langle t \rangle = \frac{\int_{-\infty}^{\infty} t |\epsilon(t)|^2 dt}{\int_{-\infty}^{\infty} |\epsilon(t)|^2 dt}$$
$$\langle \Delta \omega^2 \rangle = \frac{\int_{-\infty}^{\infty} \omega^2 |E(\omega)|^2 d\omega}{\int_{-\infty}^{\infty} |E(\omega)|^2 d\omega}$$
(11.1.4)

it can be shown that these quantities are related through the following universal inequality:

$$\boxed{\Delta t \Delta \omega \ge \frac{1}{2}} \tag{11.1.5}$$

This classical-physics relationship, which leads to the quantum-mechanical time-energy uncertainty principle, has several important consequences in the field of ultrashort light pulses.

- In order to produce a light pulse with a given duration it is necessary to use a broad enough spectral bandwidth. A Gaussian-shaped pulse lasting for one picosecond (10^{-12} s) has a minimum spectral bandwidth of 441 MHz ($\Delta\omega=4.41\times10^{11}$ Hz). If the central frequency ν_0 of the pulse lies in the visible part of the electromagnetic spectrum, say $\nu_0=4.84\times10^{14}$ Hz (wavelength $\lambda_0=620$ nm), then the relative frequency bandwidth is $\Delta\nu/\nu_0\approx10^{-3}$. But for a 100 times shorter pulse ($\Delta t=10$ fs), $\Delta\nu/\nu_0\sim0.1$. As $|\Delta\lambda/\lambda_0|=\Delta\nu/\nu_0$, the wavelength extension of this pulse is 62 nm, covering 15% of the visible window of the electromagnetic spectrum. Taking into account the wings of the spectrum, a 10 fs pulse actually covers; most of the visible window!
- Equality to 1/2 in (11.1.5) can only be reached with Gaussian time and spectral envelopes. The Gaussian pulse shape "consumes" a minimum amount of spectral components. When the equality is reached in (11.1.5), the pulse is called a Fourier-transform-limited pulse. The phase variation of such a pulse has a linear time dependence as described by (11.1.2); in other words, the instantaneous frequency is time-independent.
- For a given spectrum, one pulse envelope can be constructed that has the shortest possible duration.
- The shortest constructed pulse can only be transform-limited if its spectrum is symmetrical.
- If a transform-limited pulse is not Gaussian-shaped, then the equality in an expression similar to (11.1.5) applies, but for a constant quantity larger than 1/2 which depends on the shape of the pulse.

From the experimental point of view, half-maximum quantities are easier to measure; the Fourier inequality is then usually written as $\Delta\nu\Delta t=K$ where $\Delta\nu$ is the frequency full width at half-maximum and Δt the half maximum duration K is a number which depends on the shape of the pulse. Table 2.1 gives values of K for some symmetrical pulse shapes.

Table 11.1: Values of K for various pulse shapes, in the inequality $\Delta \nu \Delta t \geq K$, when $\Delta \nu$, and Δt are half-maximum quantities

Shape	$\epsilon(t)$	K
Gaussian function	$e^{-(t/t_0)^2/2}$	0.441
Exponential function	$e^{-(t/t_0)/2}$	0.140
Hyperbolic secant	$1/\cosh(t/t_0)$	0.315
Rectangle	_	0.892
Cardinal sine	$\sin^2(t/t_0)/(t/t_0)^2$	0.336
Lorentzian function	$[1+(t/t_0)^2]^{-1}$	0.142

Let us now consider a simple Gaussian light pulse

$$E_y = Re\left(E_0 e^{-\Gamma t^2 + i\omega_0 t}\right) \tag{11.1.6}$$

The instantaneous frequency is obtained by calculating the time derivative of the phase,

$$\omega(t) = \partial \phi / \partial t = \omega_0 \tag{11.1.7}$$

In this situation the angular frequency is constant and equals the central angular frequency ω_0 . The light pulse is transform-limited; $\Delta\nu\Delta t = 0.441$ Let us now suppose that the phase of the pulse obeys a quadratic law in time,

$$E_y = Re\left(E_0 e^{-\Gamma t^2 + i(\omega_0 t - at^2)}\right), \quad \Gamma \in \text{Re}$$
(11.1.8)

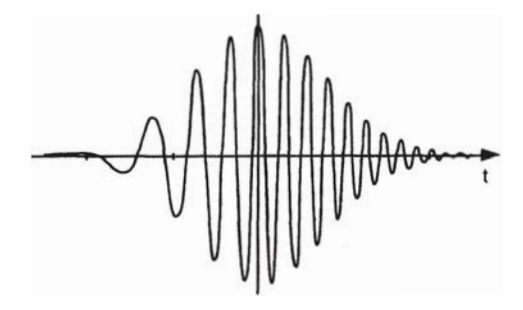


Figure 11.6: Time evolution of the electric field in a quadric pulse having a quadratic time dependence of the phase

then the instantaneous angular frequency varies linearly with time (Fig. 11.6):

$$\omega(t) = \partial \phi / \partial t = \omega_0 + \alpha t, \qquad \alpha > 0$$
 (11.1.9)

When a quadratic time dependence is added to the original phase term, the instantaneous frequency is more red in the leading part of the pulse and more blue in the trailing part (compare Fig. 11.3). The pulse is said to be "chirped". In that specific, unrealistic case its duration remains the same and its intensity spectrum has not been changed.

Introduction

After the considerations developed in the preceding chapter, it seems contradictory, a priori, to generate ultrashort pulses with a laser source, because of the frequency selection imposed by the laser cavity. Indeed, the Fourier transform of an extremely short light pulse is spectrally very broad. Yet, a laser cavity will allow oscillation in only a few very narrow frequency domains around the discrete resonance frequencies $\nu_q = qc/2L$ (where q is an integer, c the speed of light and L the optical length of the laser cavity). Therefore a laser cannot deliver ultrashort pulse while functioning in its usual regime, in which the cavity plays the part of a frequency selector. However, when a laser operates in its most usual regime, it oscillates simultaneously over all the resonance frequencies of the cavity for which the unsaturated gain is greater than the cavity losses. These frequencies make up the set of longitudinal modes of the laser. While operating in the multimode regime, the output intensity of the laser is no longer necessarily constant with time. Its time distribution depends essentially on the phase relations existing between the different modes, as illustrated by the simulation in Fig. 11.7. Figure 11.7a shows the intensity of oscillation of a single mode, Fig.11.7b that of the resultant intensity of two modes in phase, and Figs. 11.7c and d that of eight modes. In the case of Fig.11.7c, where the phase differences between the modes were chosen randomly, the time distribution of the intensity shows a random distribution of maxima. In the case of Fig. 11.7d, the eight modes oscillate with the same initial phase, and the time distribution shows a periodic repetition of a wave packet resulting from the constructive interference of the eight modes.

This very simple simulation, which can be done with a home computer, points out the importance of phase relations to the time distribution of laser intensity. This role can be very simply understood with Fresnel visualization, as shown in Fig. 11.8.

Let us assume n modes, with sinusoidal oscillation at angular frequencies ω_i with identical phases at time t=0 and with equal amplitude E ($E_i=E\sin\omega_i t$). Further, let us assume that $\omega_{i+k}-\omega_i=k\Delta\omega,k$ being an integer and $\Delta\omega$ a fixed spectral interval. At t=0, the resultant amplitude $E_T=nE$, since all the components are aligned along the x axis of the diagram (Fig. 11.8a). At some later time Δt , the representative vector has rotated through an angle equal to $\omega_i\Delta t$ and the angle difference θ between two adjacent modes will be (Fig. 11.8b);

$$\theta = \Delta\omega\Delta t \tag{11.1.10}$$

As shown in Fig. 11.8c, when $\theta = 2\pi/m$ the resultant amplitude E_T goes to zero. This occurs at time $\Delta t = \Delta \tau$, where

$$\Delta \tau = \frac{2\pi}{m\Delta\omega} \tag{11.1.11}$$

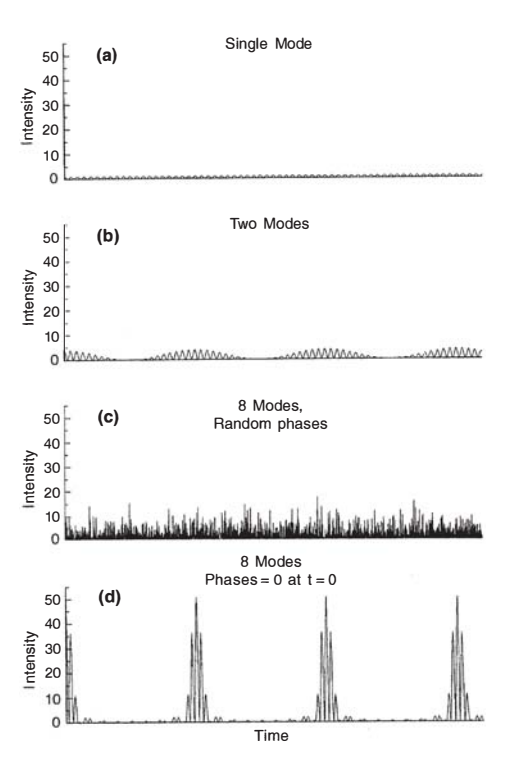


Figure 11.7: illustration of the influence of the phase relation between the modes on the resonant intensity of oscillation. (a) One mode, (b) two modes in phase, (c) eight modes with random phases, (d) eight modes with the same phase

The larger the number of modes m, the shorter is the time $\Delta \tau$ for the amplitude to go from its maximum to zero.

Each time $\theta=2k\pi$, E_T will again reach a maximum $(E_T=mE)$, and this will occur at time $T=2k\pi/\Delta\omega$ (Fig. 11.7d). To summarize, for a large number of modes m and a spectral interval $\Delta\omega$, the resultant amplitude will periodically reach its maximum, with period T, and will go to zero very fast at time $kT+\Delta\tau$. This very simple representation illustrates the role of the phase in constructive and destructive interference between the different modes. Note that if $\Delta\omega=2\pi c/2L$ then T=2L/c.

We see that the laser output will consist of a periodic sequence of pulses instead of just a single pulse. The width of each pulse will be inversely proportional to the number of modes contributing to the oscillation. The value of the period T is given by T = 2L/c.

Figure 11.9 shows a calculated simulation of this kind of behavior. Pulses which are obtained by assuming that the initial phases are rigorously equal are said to be Fourier-transform-limited and the laser is said to be "mode-locked".

The aim of this chapter is, first of all, to examine the mode-locked regime of the Laser in detail, as compared to its usual free multimode regime. We shall pay special attention to the vanous methods actually used to lock the mode phases relative to one another. In the rest of the chapter, we shall implicitly assume that all longitudinal oscillation modes are transverse fundamental TEM $_{00}$ modes. In this book, we shall not go into the phase-locking of other transverse modes, which may also give rise to interesting laser behavior.

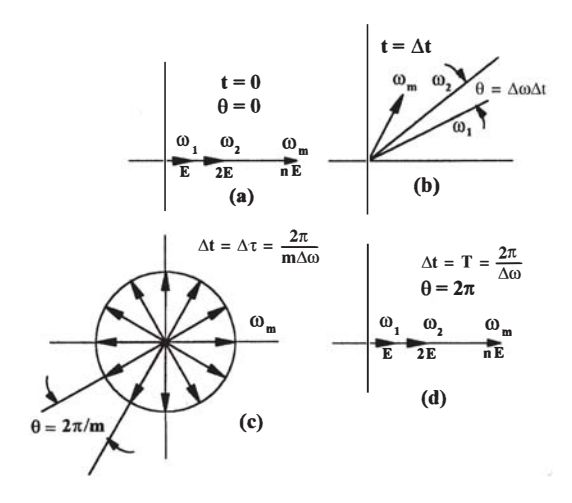


Figure 11.8: Fresnel representation of m modes. The sum of the vectors represents the amplitude of the field inside a laser cavity at different times, when all the modes are supposed to be in phase at time t = 0 (see text)

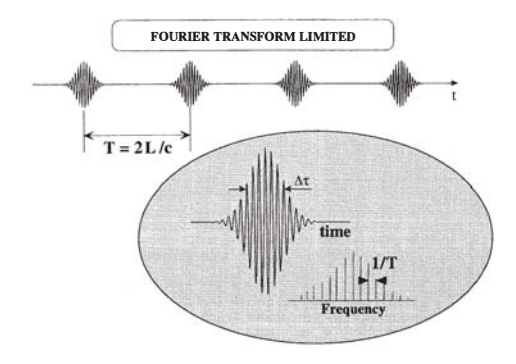


Figure 11.9: Illustration of Fourier-transform-limited pulses

11.2 Multimode lasing ³

In this section we contemplate the effect of homogeneous or inhomogeneous broadening on the laser oscillation.

We start by reminding ourselves of some basic results pertinent to this discussion:

1. The actual gain constant prevailing inside a laser oscillator at the oscillation frequency ν is clamped, at steady state, at a value that is equal to the losses

$$g_r(\nu) = \alpha - \frac{1}{l} \ln r_1 r_2$$
 (11.2.1)

where l is the length of the gain medium as well as the distance between the mirrors which are taken here to be the same.

2. The gain constant of a distributed laser medium is given, by

$$g(\nu) = (N_2 - N_1) \frac{c^2}{8\pi n^2 \nu^2 t_{\text{spont}}} \delta(\nu)$$
 (11.2.2)

 $^{^3}$ Chapter 6 (Page 201 - 212) - Optical Electronics in Modern Communications- Fifth Edition - Amnon Yariv - Oxford University Press, 1997

3. The optical resonator can support oscillations, provided sufficient gain is present to overcome losses, at frequencies ν_q separated by

$$\nu_{q+1} - \nu_q = \frac{c}{2nl} \tag{11.2.3}$$

Now consider what happens to the gain constant $g(\nu)$ inside a laser oscillator as the pumping is increased from some value below threshold. Operationally, we can imagine an extremely weak wave of frequency ν launched into the laser medium and then measuring the gain constant $g(\nu)$ as "seen" by this signal as ν is varied.

We treat first the case of a homogeneous laser. Below threshold the inversion $N_2 - N_1$ is proportional to the pumping rate and $g(\nu)$ is proportional to $\delta(\nu)$. This situation is illustrated by curve A in Figure 11.10(a). The spectrum of the passive resonances is shown in Figure 11.10(b). As the pumping rate is increased, the point is reached at which the gain per pass at the center resonance frequency ν_0 is equal to the average loss per pass. This is shown in curve B. At this point, oscillation at ν_0 starts. An increase in the pumping cannot increase the inversion since this will cause $g(\nu_0)$ to increase beyond its clamped value. Since the spectral lineshape function $\delta(\nu)$ describes the response of each individual atom, all the atoms being identical, it follows that the gain profile $g(\nu)$ above threshold as in curve C is identical to that at threshold curve B. The gain at other frequencies-such as $\nu_{-1}, \nu_1, \nu_{-2}, \nu_2$, and so forth-remains below the threshold value so that the ideal homogeneously broadened laser can oscillate only at a single frequency.

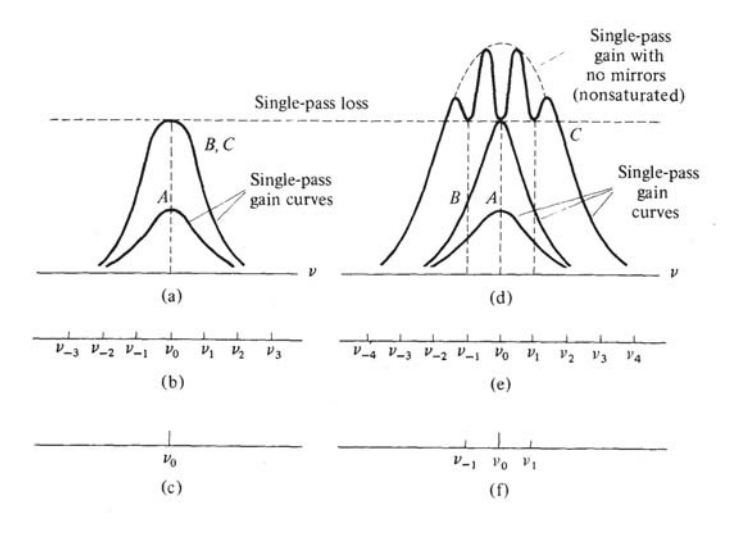


Figure 11.10: (a) Single-pass gain curves for a homogeneous atomic system (A-below threshold; B-at threshold; e-well above threshold). (b) Mode spectrum of optical resonator. (c) Oscillation spectrum (only one mode oscillates). (d) Single-pass gain curves for an inhomogeneous atomic system (A-below threshold; B-at threshold; e-well above threshold). (e) Mode spectrum of optical resonator. (f) Oscillation spectrum for pumping level e, showing three oscillating modes.

In the extreme inhomogeneous case, the individual atoms can be considered as being all different from one another and as acting independently. The lineshape function $g(\nu)$ reflects the distribution of the transition frequencies of the individual atoms. The gain profile $\gamma(\nu)$ below threshold is proportional to $g(\nu)$, and its behavior is similar to that of the homogeneous case. Once threshold is reached as in curve B, the gain at ν_0 remains clamped at the threshold value. There is no reason, however, why the gain at other frequencies should not increase with further pumping. This gain is due to atoms that do not communicate with those contributing to the gain at ν_0 . Further pumping will thus lead to oscillation at additional longitudinal-mode frequencies as shown in curve C. Since the gain at each oscillating frequency is clamped, the gain profile curve acquires depressions at the oscillation frequencies. This phenomenon is referred to as "hole burning".

⁴Further increase in pumping, and the resulting increase in optical intensity, will eventually cause a broadening of $g(\nu)$ due to the shortening of the lifetime by induced emission.

A plot of the output frequency spectrum showing the multimode oscillation of a He-Ne 0.6328- μ m laser is shown in Figure 11.11.

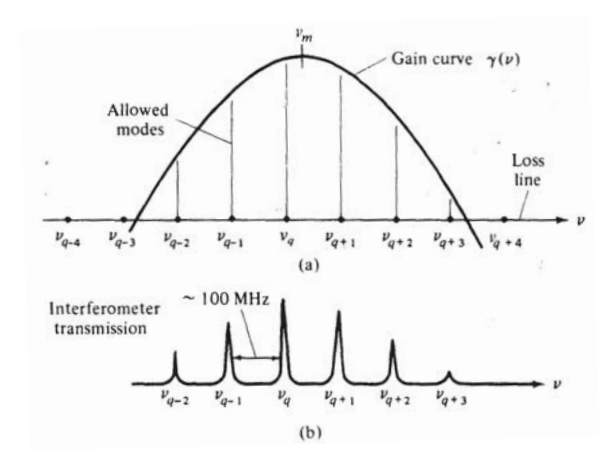


Figure 11.11: (a) Inhomogeneously broadened Doppler gain curve of the 6328 Ne transition and position of allowed longitudinal-mode frequencies. (b) Intensity versus frequency profile of an oscillating He-Ne laser. Six modes have sufficient gain to oscillate.

Mode Locking

We have argued above that in an inhomogeneously broadened laser, oscillation can take place at a number of frequencies, which are separated by (assuming n = 1)

$$\omega_q - \omega_{q-1} = \frac{\pi c}{I} \equiv \omega \tag{11.2.4}$$

Now consider the total optical electric field resulting from such multimode oscillation at some arbitry point, say next to one of the mirrors, in the optical resonator. It can be taken, using complex notation, as

$$e(t) = \sum_{n} E_n e^{i[(\omega_0 + n\omega)t + \phi_n]}$$
(11.2.5)

where the summation is extended over the oscillating modes and ω_0 is chosen, arbitrarily, as a reference frequency. ϕ_n is the phase of the *n*th mode. One property of (11.2.5) is that e(t) is periodic in $T = 2\pi/\omega = 2l/c$, which is the round-trip transit time inside the resonator

$$e(t+T) = \sum_{n} E_{n} \exp\left\{i\left[(\omega_{0} + n\omega)\left(t + \frac{2\pi}{\omega}\right) + \phi_{n}\right]\right\}$$

$$= \sum_{n} E_{n} \exp\left\{i\left[(\omega_{0} + n\omega)t + \phi_{n}\right]\right\} \exp\left\{i\left[2\pi\left(\frac{\omega_{0}}{\omega} + n\right)\right]\right\}$$

$$= e(t)$$
(11.2.6)

Since ω_0/ω is an integer $(\omega_0 = m\pi c/l)$,

$$e^{2\pi i \left(\frac{\omega_0}{\omega} + n\right)} = 1\tag{11.2.7}$$

Note that the periodic property of e(t) depends on the fact that the phases ϕ_n are fixed. In typical lasers the phases ϕ_n are likely to vary randomly with time. This causes the intensity of the laser output to fluctuate randomly⁵ and greatly reduces its usefulness for many applications where temporal coherence is important.

 $^{^{5}}$ It should be noted that this fluctuation takes place because of random interference between modes and not because of intensity fluctuations of individual modes.

Two ways in which the laser can be made coherent are: First, make it possible for the laser to oscillate at a single frequency only so that mode interference is eliminated. This can be achieved in a variety of ways, including shortening the resonator length l, thus increasing the mode spacing $(\omega = \pi c/l)$ to a point where only one mode has sufficient gain to oscillate. The second approach is to force the modes' phases ϕ_n to maintain their relative values. This is the so-called "mode locking" technique proposed and demonstrated in the early history of the laser. This mode locking causes the oscillation intensity to consist of a periodic train with a period of $T = 2l/c = 2\pi/\omega$.

One of the most useful forms of mode locking results when the phases ϕ_n are made equal to zero. To simplify the analysis of this case, assume that there are N oscillating modes with equal amplitudes. Taking $E_n = 1$ and $\phi_n = 0$ in (11.2.5) gives

$$e(t) = \sum_{n=-(N-1)/2}^{(N-1)/2} e^{i(\omega_0 + n\omega)t}$$

$$= e^{i\omega_0 t} \frac{\sin(N\omega t/2)}{\sin(\omega t/2)}$$
(11.2.8)

The average laser power output is proportional to $e(t)e^*(t)$ and is given by ⁶

$$P(t) \propto \frac{\sin^2(N\omega t/2)}{\sin^2(\omega t/2)}$$
(11.2.9)

Some of the analytic properties of P(t) are immediately apparent:

- 1. The power is emitted in a form of a train of pulses with a period $T=2\pi/\omega=2l/c$, i.e., the round-trip delay time.
- 2. The peak power, P(sT) (for s = 1, 2, 3, ...), is equal to N times the average power, where N is the number of modes locked together.
- 3. The peak field amplitude is equal to N times the amplitude of a single mode.
- 4. The individual pulse width, defined as the time from the peak to the first zero is $\tau_0 = T/N$. The number of oscillating modes can be estimated by $N \simeq \Delta \omega/\omega$ -that is, the ratio of the transition lineshape width $\Delta \omega$ to the frequency spacing ω between modes. Using this relation, as well as $T = 2\pi/\omega$ in $\tau_0 = T/N$, we obtain

$$\tau_0 \sim \frac{2\pi}{\Delta\omega} = \frac{1}{\Delta\nu} \tag{11.2.10}$$

Thus the length of the mode-locked pulses is approximately the inverse of the gain linewidth

A theoretical plot of $\sqrt{P(t)}$ as given by (11.2.9) for the case of five modes (N=5) is shown in Figure 11.12. The ordinate may also be considered as being proportional to the instantaneous field amplitude.

The foregoing discussion was limited to the consideration of mode locking as a function of time. It is clear, however, that since the solution of Maxwell's equations in the cavity involves traveling waves (a standing wave can be considered as the sum of two waves traveling in opposite directions), mode locking causes the oscillation energy of the laser to be condensed into a packet that travels back and forth between the mirrors with the velocity of light c. The pulsation period T=2l/c corresponds simply to the time interval between two successive arrivals of the pulse at the mirror. The spatial length of the pulse L_p must correspond to its time duration multiplied by its velocity c. Using $\tau_0=T/N$ we obtain

$$L_p \sim c\tau_0 = \frac{cT}{N} = \frac{2\pi c}{\omega N} = \frac{2l}{N}$$
 (11.2.11)

⁶The averaging is performed over a time that is long compared with the optical period $2\pi/\omega_0$ but short compared with the modulation period $2\pi/\omega$.

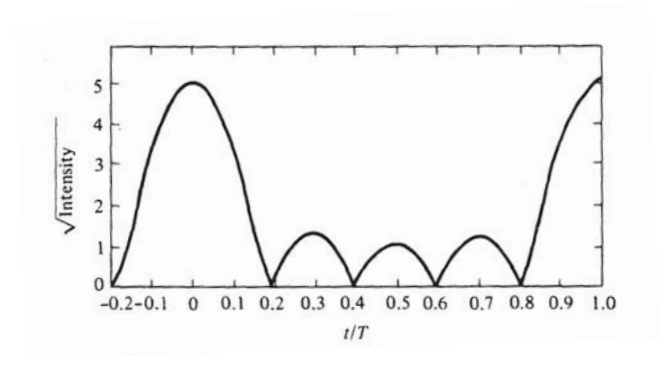


Figure 11.12: Theoretical plot of optical field amplitude $\sqrt{P(t)} \propto |\sin(N\omega t/2)\sin(\omega t/2)|$ resulting from phase locking of five (N=5) equal-amplitude modes separated from each other by a frequency interval $\omega = 2\pi/T$.

We can verify the last result by taking the basic resonator mode as a standing wave $\sin k_n z \sin \omega_n t$; the total optical field is then

$$e(z,t) = \sum_{n=-(N-1)/2}^{(N-1)/2} \sin\left[\frac{(m+n)\pi}{l}z\right] \sin\left[(m+n)\frac{\pi c}{l}t\right]$$
(11.2.12)

where $\omega_n = (m+n)(\pi c/l)$, $k_n = \omega_n/c$, and m is the integer (equal to the number of half wavelengths $m = l/(\lambda/2)$) corresponding to the central mode. We can rewrite (11.2.12) as

$$e(z,t) = \frac{1}{2} \sum_{n=-(N-1)/2}^{(N-1)/2} \left\{ \cos\left[(m+n)\frac{\pi}{l}(z-ct) \right] - \cos\left[(m+n)\frac{\pi}{l}(z+ct) \right] \right\}$$
(11.2.13)

which can be shown to have the spatial and temporal properties described previously. Figure 11.13 shows a spatial plot of (11.2.13) at time t.

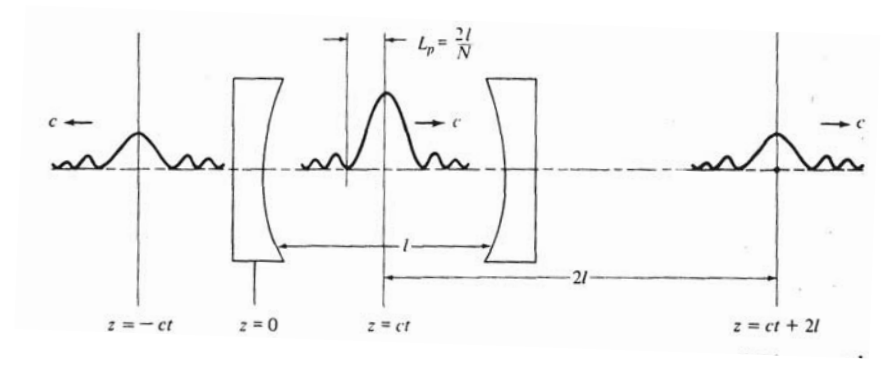


Figure 11.13: Traveling pulse of energy resulting from the mode locking of N laser modes; based on Equation (11.2.13).

Methods of Mode Locking

In the preceding discussion we considered the consequences of fixing the phases of the longitudinal modes of a laser-mode locking. Mode locking can be achieved by modulating the losses (or gain) of the laser at a radian frequency $\omega = \pi c/l$, which is equal to the intermode frequency spacing. The theoretical proof of mode locking by loss modulation is rather formal, but a good plausibility argument can be made as follows: As a form of loss modulation consider a thin shutter inserted

inside the laser resonator. Let the shutter be closed (high optical loss) most of the time except for brief periodic openings for a duration of τ_{open} every T = 2l/c seconds. This situation is illustrated by Figure 11.14. A single laser mode will not oscillate in this case because of the high losses (we

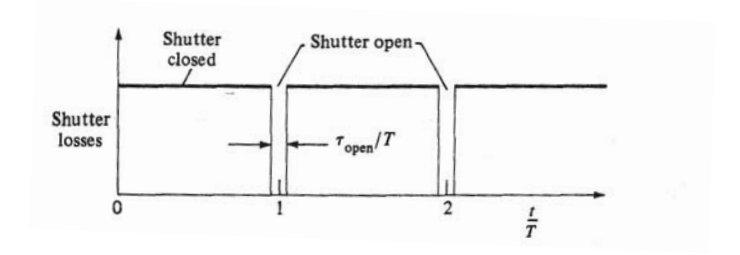


Figure 11.14: Periodic losses introduced by a shutter to induce mode locking. The presence of these losses favors the choice of mode phases that results in a pulse passing through the shutter during open intervals-that is, mode locking.

assume that $\tau_{\rm open}$ is too short to allow the oscillation to build up during each opening). The same applies to multimode oscillation with arbitrary phases. There is one exception, however. If the phases were "locked" as in (11.2.8), the energy distribution inside the resonator would correspond to that shown in Figure 11.13 and would consist of a narrow ($L_p = 2l/N$) traveling pulse. If this pulse should arrive at the shutter's position when it is open and if the pulse (temporal) length τ_0 is short compared to the opening time $\tau_{\rm open}$, the mode-locked pulse will be "unaware" of the shutter's existence and, consequently, will not be attenuated by it. We may thus reach the conclusion that loss modulation causes mode locking through some kind of "survival of the fittest" mechanism. In reality the periodic shutter chops off any intensity tails acquired by the mode-locked pulses due to a "wandering" of the phases from their ideal ($\phi_n = 0$) values. This has the effect of continuously restoring the phases.

An experimental setup used to mode-lock a He-Ne laser is shown in Figure 11.15; the periodic loss is introduced by Bragg diffraction of a portion of the laser intensity from a standing acoustic wave. The standing-wave nature of the acoustic oscillation causes the strain to have a form

$$S(z,t) = S_0 \cos \omega_a t \cos k_a z \tag{11.2.14}$$

where the acoustic velocity is $v_a = \omega_a/k_a$. Since the change in the index of refraction is to first order, proportional to the strain S(z,t), we can interpret (11.2.14) as a phase diffraction grating with a spatial period $2\pi/k_a$, which is equal to the acoustic wavelength. The diffraction loss of the incident laser beam due to the grating reaches its peak twice in each acoustic period when S(z,t) has its maximum and minimum values. The loss modulation frequency is thus $2\omega_a$, and mode locking occurs when $2\omega_a = \omega$, where ω is the (radian) frequency separation between two longitudinal laser modes.

Figure 11.16 shows the pulses resulting from mode locking a Rhodamine 6 G dye laser.

Mode locking occurs spontaneously in some lasers if the optical path contains a saturable absorber (an absorber whose opacity decreases with increasing optical intensity). This method is used to induce mode locking in the high-power pulsed solid-state lasers and in continuous dye lasers. This is due to the fact that such a dye will absorb less power from a mode-locked train of pulses than from a random phase oscillation of many modes, since the first form of oscillation leads to the highest possible peak intensities, for a given average power from the laser, and is consequently attenuated less severely. From arguments identical with those advanced in connection with the periodic shutter, it follows that the presence of a saturable absorber in the laser cavity will "force" the laser, by a "survival of the fittest" mechanism, to lock its modes' phases as in (11.2.13).

Some of the shortest mode-locked pulses to date were obtained from dye lasers employing Rhodamine 6G as the gain medium. The mode locking is caused by synchronous gain modulation that is due to the fact that the pumping (blue-green) argon gas laser is itself mode-locked. The pump pulses are synchronized exactly to the pulse repetition rate of the dye laser. (This requires that both lasers have precisely the same optical length.) When this is done, the dye laser gain medium will be pumped once in each round-trip period so that the pumping pulse and the mode locked pulse overlap spatially and temporally in the dye cell.

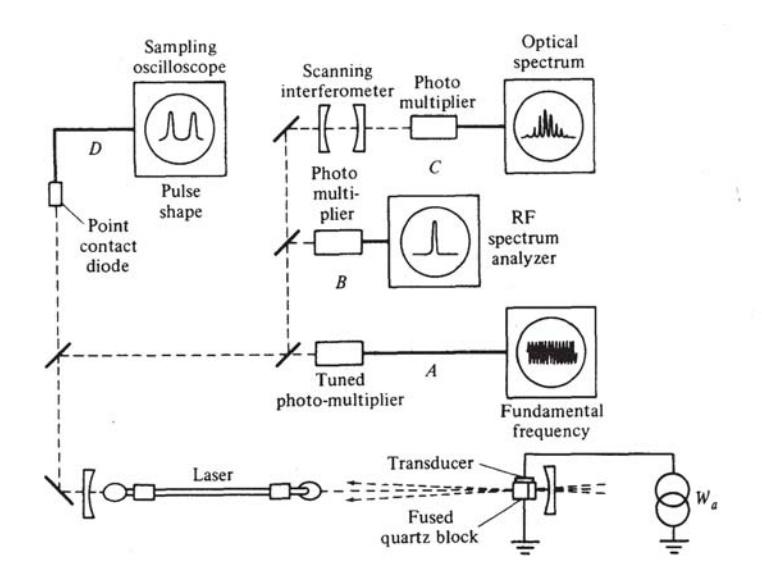


Figure 11.15: Experimental setup for laser mode locking by acoustic (Bragg) loss modulation. The loss is due to Bragg diffraction of the main laser beam by a standing acoustic wave. Parts A, B, C, and D of the experimental setup are designed to display the fundamental component of the intensity modulation, the power spectrum of the intensity modulation, the power spectrum of the optical field e(t), and the optical intensity, respectively.

Additional sharpening of the mode-locked pulses can result from the inclusion of a saturable (dye) absorber in the resonator.

A sketch of a synchronously mode-locked dye laser configuration is shown in Figure 6-16.

Additional amplification of the output pulses qf the dye laser by a sequence of three to four dye laser amplifier cells (consisting of Rhodamine 6G pumped by the pulsed second harmonic of Q-switched Nd³⁺: YAG lasers) has yielded subpicosecond pulses with peak power exceeding 10^9 watts.

The shortest pulses obtained to date are $\sim 30 \times 10^{-15}$ s. These pulses have been narrowed down further to $\sim 6 \times 10^{-15}$ s by the use of nonlinear optical techniques.

Ultrashort mode-locked pulses are now used in an ever-widening circle of applications involving the measurement and study of short-lived molecular and electronic phenomena. The use of ultrashort optical pulses has led to an improvement of the temporal resolution of such experiments by more than three orders of magnitude. For a description of many of these applications as well as of the many methods used to measure the pulse duration, the student should consult References.

Mode locking in semiconductor lasers is of particular interest owing to the very large gain bandwidth in these media. These lasers offer potential operation in the 10-20 femtosecond range although present results are far of this goal. Of special interest is the possibility of controlling the gain and loss by means of multiple electrodes.

Table 11.2 lists some of the lasers commonly used in mode locking, along with the achievable pulse durations.

11.3 Phase locked oscillators ⁷

We will consider the problem of adding the displacements of N harmonic oscillators with equally spaced frequencies. That is, we consider the sum of

$$x_n(t) = x_0 \sin(\omega_n t + \phi_0) \tag{11.3.1}$$

 $^{^7{\}rm Chapter}$ 6 (Pages 239 - 246) - Laser Physics - Peter W. Milonni, Joseph H. Eberly - Hoboken, New Jersey : John Wiley & Sons Ltd, 2010

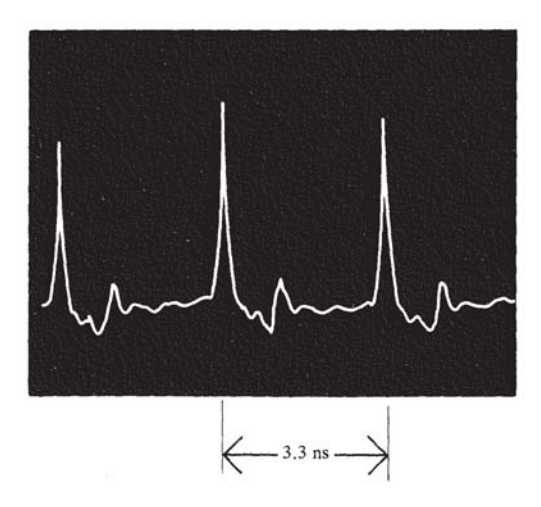


Figure 11.16: Power output as a function of time of a mode-locked dye laser, using Rhodamine 6G. The oscillation is at $\lambda = 0.61 \mu m$. The pulse width is detector limited

Table 11.2: Some Laser Systems, Their Gain Linewidth $\Delta \nu$, and the Length of Their Pulses in the Mode-Locked Operations

	$\Delta \nu$	$\Delta \nu^{-1}$,	Observed Pulse Duration
Laser Medium	Hz	Seconds	$ au_0$ Seconds
He-Ne	$\sim 1.5 \times 10^9$	6.66×10^{-10}	$\sim 6 \times 10^{-10}$
$(0.6328 \mu m)$			
CW			
Nd:YAG	$\sim 1.2 \times 10^{10}$	8.34×10^{-11}	$\sim 7.6 \times 10^{-11}$
$(0.6328 \mu m)$			
ĊW			
Ruby	6×10^{10}	1.66×10^{-11}	$\sim 1.2 \times 10^{-11}$
$(0.6328 \mu m)$			
pulsed			
Nd ³⁺ :glass	3×10^{12}	3.33×10^{-13}	3×10^{-13}
pulsed			
Rhodamine 6G	10^{13}	10^{-13}	3×10^{-14}
(dye laser)(0.6 μ m)			
Diode lasers	10^{13}	10^{-13}	4×10^{-13}

where

$$\omega_n = \omega_0 + n\Delta, \qquad n = -\frac{N-1}{2}, -\frac{N-1}{2} + 1, -\frac{N-1}{2} + 2, \dots, \frac{N-1}{2}$$
 (11.3.2)

In other words, the amplitudes x_0 and phases ϕ_0 of the oscillators are identical, and their frequencies ω_n are equally spaced by Δ and centered at ω_0 , as shown in Fig. 11.18. The sum of the displacements is

$$X(t) = \sum_{n} x_n(t) = -\sum_{-(N-1)/2}^{(N-1)/2} x_0 \sin(\omega_n t + \phi_0)$$
(11.3.3)

Since $\sin x$ is the imaginary part of e^{ix} , we may write this as

$$X(t) = x_o \operatorname{Im}\left(\sum_{n} e^{i(\omega_0 t + \phi_0 + n\Delta t)}\right) = x_o \operatorname{Im}\left(e^{i(\omega_0 t + \phi_0)} \sum_{n} e^{in\Delta t}\right)$$
(11.3.4)

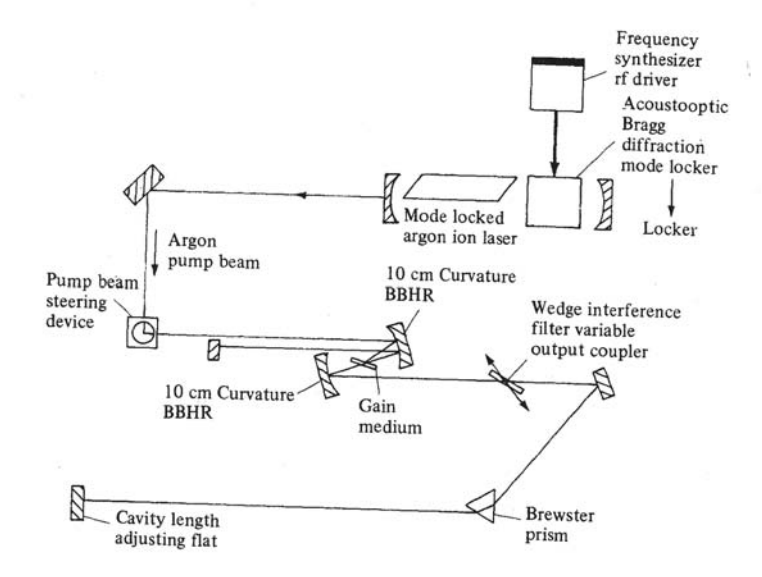


Figure 11.17: Synchronously mode-locked dye laser configuration.



Figure 11.18: A collection of N frequencies running from $\omega_0 - \frac{1}{2}(n = N - 1)\Delta$ to $\omega_0 + \frac{1}{2}(N - 1)\Delta$ as in Eq. (11.3.2).

The general identity

$$\sum_{n=-(N-1)/2}^{(N-1)/2} e^{iny} = \frac{\sin(Ny/2)}{\sin(y/2)}$$
 (11.3.5)

proved below allows us to write (11.3.4) as

$$X(t) = x_0 \operatorname{Im} \left[e^{i(\omega_0 t + \phi_0)} \frac{\sin(N\Delta t/2)}{\sin(\Delta t/2)} \right] = x_0 \sin(\omega_0 t + \phi_0) \left[\frac{\sin(N\Delta t/2)}{\sin(\Delta t/2)} \right]$$
$$= A_N x_0 \sin(\omega_0 t + \phi_0)$$
(11.3.6)

The function $A_N(t)$ is plotted in Fig. 11.19 for N=3 and N=7. In general $A_N(t)$ has equal maxima

$$A_N(t)_{max} = N \tag{11.3.7}$$

at values of t given by

$$t_m = m\left(\frac{2\pi}{\Delta}\right) \equiv mT, \qquad m = 0, \pm 1, \pm 2, \dots$$
 (11.3.8)

As N increases, the maxima of $A_N(t)$ become larger. They also become more sharply peaked. A measure of their width is the time interval τ_N indicated in Fig. 11.19 for N=7:

$$\tau_N = \frac{2\pi}{N\Delta} = \frac{T}{N} \tag{11.3.9}$$

We have thus shown that the addition of N oscillators of equal amplitudes and phases, and equally spaced frequencies 11.3.2, gives maximum total oscillation amplitudes equal to N times the amplitude of a single oscillator. These maximum amplitudes occur at intervals of time T [Eq.

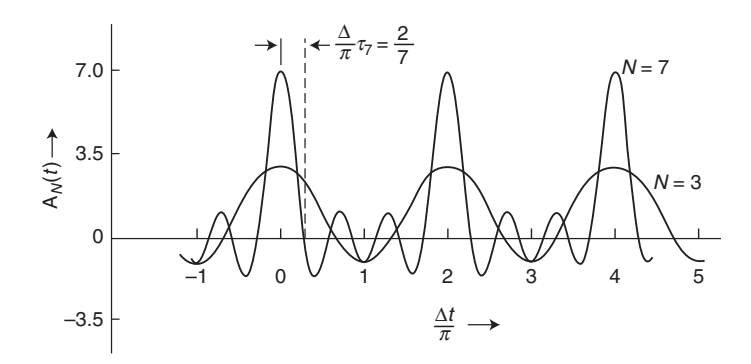


Figure 11.19: The function $A_N(t) = \sin(\frac{1}{2}N\Delta t)/\sin(\frac{1}{2}\Delta t)$ vs. $\Delta t/\pi$

(11.3.8)]. For large N we have, loosely speaking, a series of large-amplitude "spikes." The smaller the frequency spacing Δ between the individual oscillators, the larger the time interval $T=2\pi/\Delta$ between spikes, and conversely. The temporal duration of each spike is $\tau_N=T/N$, so the spikes get sharper as N is increased.

We have assumed for simplicity that each oscillator has the same phase ϕ_0 [Eq. (11.3.1)]. A more general kind of phase locking occurs when the phase differences of the oscillators are constant but not necessarily zero:

$$\phi_n = \phi_0 + n\alpha \tag{11.3.10}$$

or

$$\phi_{n+1} - \phi_n = \alpha \tag{11.3.11}$$

In this case the sum of the oscillator displacements (11.3.3) is replaced by

$$X(t) = \sum_{n} x_0 \sin(\omega_n t + \phi_n) = x_0 \operatorname{Im} \left(e^{i(\omega_0 t + \phi_0)} \sum_{-(N-1)/2}^{(N-1)/2} e^{in(\Delta t + \alpha)} \right)$$
(11.3.12)

and this may be evaluated to give the total displacement

$$X(t) = x_0 \sin(\omega_0 t + \phi_0) \left[\frac{\sin N(\Delta t + \alpha)/2}{\sin(\Delta t + \alpha)/2} \right]$$
 (11.3.13)

having basically the same properties as (11.3.6) obtained with $\alpha = 0$.

• We prove (11.3.5) as follows. Let the sum be denoted S_N . For convenience we will first evaluate

$$S_{N+1} = \sum_{n=-N/2}^{+N/2} e^{iny} \tag{11.3.14}$$

The first step is to shift the summation label by introducing

$$m = n + \frac{N}{2} \tag{11.3.15}$$

so that

$$S_{N+1} = \sum_{m=0}^{N} e^{i(m-N/2)y} = e^{-iNy/2} \sum_{m=0}^{N} e^{imy} = e^{-iNy/2} \sum_{m=0}^{N} (e^{iy})^m$$
(11.3.16)

The second step is to make use of the identity

$$\sum_{m=0}^{N} x^m = \frac{1 - x^{N+1}}{1 - x} \tag{11.3.17}$$

Then we can write

$$S_{N+1} = e^{-iNy/2} \frac{1 - e^{i(N+1)y}}{1 - e^{iy}}$$

$$= e^{-iNy/2} \frac{e^{i(N+1)y/2}}{e^{iy/2}} \frac{e^{-i(N+1)y/2} - e^{i(N+1)y/2}}{e^{-iy/2} - e^{iy/2}} = \frac{\sin(N+1)y/2}{\sin y/2}$$
(11.3.18)

and so we have proved that

$$S_N = \frac{\sin Ny/2}{\sin y/2} \tag{11.3.19}$$

as claimed in (11.3.5).

11.4 Mode Locking

What we have in the example of the preceding section is a simple model of a mode-locked laser. The individual oscillators in the model play the role of individual longitudinal-mode fields, while their frequency spacing Δ represents the mode (angular) frequency separation $2\pi(c/2L) = \pi c/L$. The assumption of equal oscillator phase differences α ("phase locking") in the model corresponds to the locking together of the phases of the different cavity modes.

Our oscillator model suggests that, if we can somehow manage to lock together the phases of N longitudinal modes of a laser, then the output light of the laser will consist of a train of pulses separated in time by $T=2\pi/\Delta=2L/c$. The temporal duration of each pulse in the train will be $\tau_N=T/N=2L/cN$. The larger the number N of phase-locked modes, the greater the amplitude, and the shorter the duration, of each individual pulse in the train. As we will see, this is indeed the essence of the mode-locking technique for obtaining very short, powerful laser pulses.

$$-\frac{1}{2}(N-1)\frac{\pi c}{L} \qquad -\frac{\pi c}{L} \qquad +\frac{\pi c}{L} \qquad -\frac{1}{2}(N-1)\frac{\pi c}{L}$$

$$\frac{M\pi c}{I}$$

Figure 11.20: The distribution of N cavity mode frequencies. The situation is exactly the same as in Fig. 11.19 for the case of N phase-locked oscillators.

The number of longitudinal modes that can simultaneously lase is determined by the gain linewidth (FWHM) $\Delta\nu_g$ and the frequency separation c/2L between modes (cf. Fig. 11.20). Under sufficiently strong pumping of the gain medium we expect that approximately

$$M = \frac{\Delta \nu_g}{c/2L} = \frac{2L}{c} \Delta \nu_g \tag{11.4.1}$$

longitudinal modes can oscillate simultaneously. The shortest pulse length we expect to achieve by mode locking is therefore

$$\tau_{\min} = \tau_M = \frac{2L}{cM} = \frac{1}{\Delta \nu_g} \tag{11.4.2}$$

That is, the shortest pulse duration we can achieve by mode locking is (approximately) the reciprocal of the gain linewidth.

Example: He-Ne Shortest possible pulse

As an example, consider the 632.8-nm HeNe laser with a gain linewidth $\Delta\nu_g=\delta\nu_D=1700$

MHz. For such a laser the shortest pulses obtainable by mode locking are of duration

$$\frac{1}{\delta\nu_D} = \frac{1}{1700 \times 10^6} s^{-1} = 1$$
ns (11.4.3)

In other words, for this laser, mode locking is not much of an improvement over Q switching for the production of short pulses. This is often true of gas lasers. Their gain linewidths are so narrow that very short (say, picosecond, 10^{-12} s duration) pulses cannot be obtained by mode locking.

On the other hand, consider a 693.4-nm ruby laser with $\Delta\nu_g\approx 10^{11}~{\rm s}^{-1}$. For this laser mode-locked pulses of 10^{-11} s may be obtained.

Liquid dye lasers typically have broad gain profiles, with $\Delta \nu_g \approx 10^{12} \text{ s}^{-1}$ or more. With such lasers mode-locked pulses in the picosecond range are routinely obtained.

A basic understanding of mode-locked laser oscillation may be reached by extending only slightly our analysis of phase-locked oscillators. We associate with the *m*th longitudinal mode an electric field

$$E(z,t) = \hat{\epsilon}E_m(z)\sin(\omega_m t + \phi_m) = \hat{\epsilon}E_m\sin k_m z\sin(\omega_m t + \phi_m)$$
(11.4.4)

where

$$k_m = m\frac{\pi}{L}, \qquad m = 1, 2, 3, \dots$$
 (11.4.5a)

$$\omega_m = k_m c = m \frac{\pi c}{L}, \qquad m = 1, 2, 3, \dots$$
 (11.4.5b)

For simplicity let us assume that the mode fields all have the same magnitude (E_0) and polarization, so that we can do our calculations with scalar quantities. Furthermore let us consider, without much loss of generality, the simplest example of phase locking, in which all $\phi_m = 0$. Then the total electric field in the cavity is

$$E(z,t) = \sum_{m} E_m(z,t) = E_0 \sum_{m} \sin k_m z \sin \omega_m t$$
 (11.4.6)

where the summation is over all oscillating modes.

For a cavity 1 m long, $\pi c/L \approx 9 \times 10^8$ Hz. For near-optical frequencies, of course, the lasing frequencies ω_m will be much larger; at a wavelength of 600 nm, $\omega = 2\pi c/\lambda = 3 \times 10^{15}$ Hz. The integer m in (11.4.5) will therefore typically be in the millions. So let us take $m \to M + n$ and write equations (11.4.5) as

$$k_m = \frac{(M+n)\pi}{L} \tag{11.4.7a}$$

$$\omega_m = \frac{(M+n)\pi c}{L} \tag{11.4.7b}$$

where M is a very large positive integer $(M \approx 10^6)$ and n runs from $-\frac{1}{2}(N-1)$ to $+\frac{1}{2}(N-1)$, corresponding to a total of $N(\ll M)$ modes centered at the frequency $M\pi c/L$ (Fig. 11.20). Then (11.4.7) becomes

$$E(z,t) = E_0 \sum_{n=-(N-1)/2}^{(N-1)/2} \sin \frac{(M+m)\pi z}{L} \sin \frac{(M+m)\pi ct}{L}$$

$$= \frac{1}{2} E_0 \sum_{n} \left[\cos \frac{(M+m)\pi (z-ct)}{L} - \cos \frac{(M+m)\pi (z+ct)}{L} \right]$$
(11.4.8)

for the total electric field in the laser cavity.

Now we proceed as in the preceding section. The sum

$$\sum_{n=-(N-1)/2}^{(N-1)/2} \cos \frac{(M+n)\pi(z-ct)}{L} = \operatorname{Re} \left\{ \sum_{-(N-1)/2}^{(N-1)/2} e^{i(M+n)\pi(z-ct)/L} \right\}$$

$$= \operatorname{Re} \left\{ e^{iM\pi(z-ct)/L} \frac{\sin[\pi N(z-ct)/2L]}{\sin[\pi(z-ct)/2L]} \right\}$$

$$= \left[\cos \frac{M\pi(z-ct)}{L} \right] \frac{\sin[\pi N(z-ct)/2L]}{\sin[\pi(z-ct)/2L]}$$
(11.4.9)

where we have again used the identity (11.3.5). Similarly

$$\sum_{n} \cos \frac{(M+n)\pi(z+ct)}{L} = \left\{ \cos \frac{M\pi(z+ct)}{L} \frac{\sin[\pi N(z+ct)/2L]}{\sin[\pi(z+ct)/2L]} \right\}$$
(11.4.10)

From (11.4.8), then,

$$E(z,t) = \frac{E_0}{2} \left\{ \cos k_0(z - ct) \frac{\sin[\pi N(z + ct)/2L]}{\sin[\pi(z + ct)/2L]} - \cos k_0(z + ct) \frac{\sin[\pi N(z + ct)/2L]}{\sin[\pi(z + ct)/2L]} \right\}$$
(11.4.11)

where $k_0 = \pi M/L$.

The functions

$$A_N^{(\pm)}(z,t) = \frac{\sin[\pi N(z \pm ct)/2L]}{\sin[\pi(z \pm ct)/2L]}$$
(11.4.12)

169

appearing in (11.4.11) have basically the same form and effect as the function $A_N(t)$ appearing in Eq. (11.3.6) for the phase-locked oscillator model. In particular, $A_N^{\pm}(z,t)$ has maxima occurring at

$$a \pm ct = m(2L), \qquad m = 0, \pm 1, \pm 2, \dots$$
 (11.4.13)

If we put our attention on a fixed value of z inside the cavity, for instance, there are pulses of peak amplitude $NE_0 = 2$ appearing at time intervals of 2L/c, each pulse having a duration T/N (Fig. 11.21). If we fix our attention on the spatial distribution of E(z,t) at a fixed time t, we find pulses of amplitude $NE_0 = 2$ with spatial separation 2L, each pulse having a spatial extent of 2L/N (Fig. 11.22).

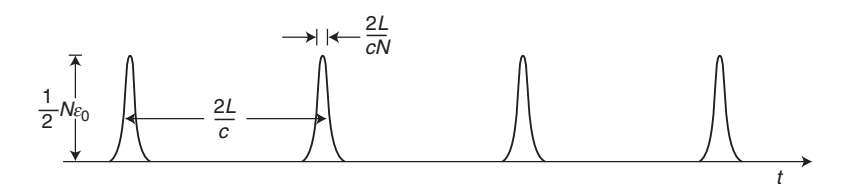


Figure 11.21: A mode-locked pulse train as a function of time, observed at a fixed position z.

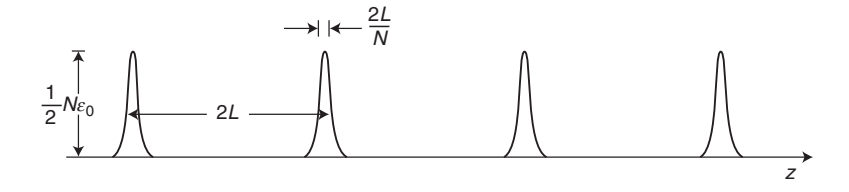


Figure 11.22: A mode-locked pulse train as a function of coordinate z, observed at a fixed instant of time.

In other words, the field (11.4.11) represents two trains of pulses, one moving in the positive z direction and the other in the negative z direction. In the usual situation in which output is

obtained through one of the cavity mirrors, the laser radiation appears as a single train of pulses of temporal separation and duration 2L/c and 2L/cN, respectively. All this confirms our conclusions deduced from the phase-locked oscillator model.

The fact that the pulses of a mode-locked train are separated in time by the round-trip cavity transit time 2L/c suggests a "bouncing-ball" picture of a mode-locked laser: We can regard the mode locking as generating a pulse of duration 2L/cN, and this pulse keeps bouncing back and forth between the cavity mirrors. Focusing our attention on a particular plane of constant z in the resonator, we observe a train of identical pulses moving in either direction.

In most lasers the phases ϕ_n of the different modes will undergo random and uncorrelated variations in time. In this case the total intensity is the sum of the individual mode intensities. In mode-locked lasers, however, the mode phases are correlated and the total intensity is not simply the sum of the individual mode intensities. In fact, the individual pulses in the mode-locked train have an intensity N times larger than the sum of the individual mode intensities. The average power, however, is essentially unaltered by mode locking the laser.

• Before discussing how mode locking can be accomplished, it is worth noting that phase locking or "synchronization" phenomena occur in many nonlinear oscillatory systems besides lasers, and indeed these phenomena have been known for a very long time. C. Huygens (1629-1695), for instance, observed that two pendulum clocks hung a few feet apart on a thin wall tend to have their periods synchronized as a result of their small coupling via the vibrations of the wall. Near the end of the 19th century, Lord Rayleigh found that two organ pipes of slightly different resonance frequencies will vibrate at the same frequency when they are sufficiently close together. The contractive pulsations of the heart's muscle cells become phase-locked during the development of the fetus. Fibrillation of the heart occurs when they get out of phase for some reason and results in death unless the heart can be shocked back into the normal condition of cell synchronization. There are other biological examples of phase locking, but detailed theoretical analyses are obviously extremely difficult or impossible for such complex systems. Modern applications of synchronization principles are made in high-precision motors and control systems. •

11.5 Passive Mode Locking by saturable absorbers ⁸

The dynamics of the gain saturation in the amplifying medium are responsible for distorting the pulse shape. Now we want to show that if an absorbing medium with a saturable absorption coefficient (Fig. 11.23) is placed inside the cavity, the association between this saturable absorber and the saturable amplifying medium leads to a natural mode-locking of the laser, without any need for external monitoring. The most commonly used saturable absorbers usually consist of liquid dye solutions. However, especially since the advent of Ti:sapphire lasers, an active search is going on to find solid media which could serve as saturable absorbers, especially among the semiconductors.

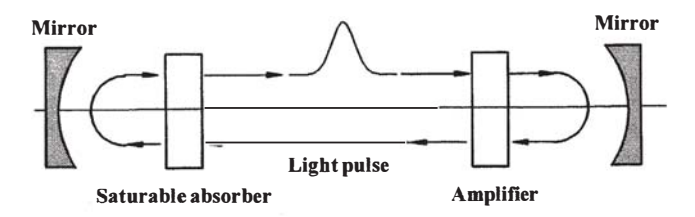


Figure 11.23: Round-trip pulse in a laser cavity including saturable absorber and amplifying medium.

This mode-locking process is simpler to explain in the time domain. Let us look at the transmission characteristics of a saturable absorber. At low incident intensity, the transmission T stays

⁸Chapter 3 (Page 70 - 73) - Femtosecond laser pulses : principles and experiments -Rulliere, Claude - New York : Springer, 2005

practically constant, with a value of T_0 which is almost independent of the incident intensity (Fig. 11.24). But if the incident intensity increases, the population of the upper level involved in the absorption process increases, as does the stimulated emission from this level. At the same time, the population of the lower level decreases.

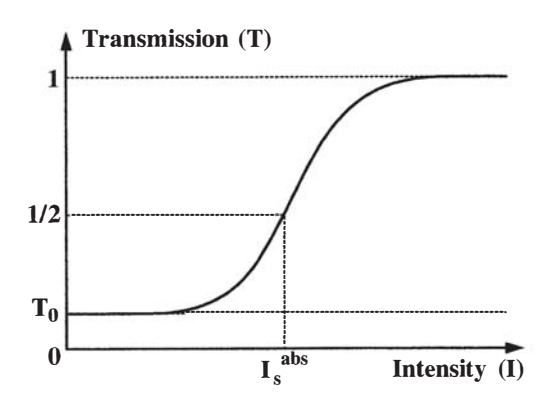


Figure 11.24: Transmission through a saturable absorber as a function of the input intensity

The combination of these two effects results in a nonlinear behavior of the transmission coefficient, as shown in Fig. 11.24. The absorber is characterized by its saturation intensity I_s^{abs} . This parameter is defined as the intensity at which the population difference that exists between the two levels at low intensity is reduced by a factor of two. This definition thus implies that the absorption coefficient α must be proportional to the population difference.

Moreover, as was said earlier, the amplifying medium also possesses saturation properties. At low intensity, the gain G has a constant value G_0 , which is rather large (Fig. 11.25). It is said to be unsaturated. At higher input intensities, there is a lessening of the population inversion between the two levels involved in the process, and the gain G decreases. As can be seen in Fig. 11.25, we can define I_s^{amp} , the saturation intensity for G, in an equivalent way to the saturation intensity I_s^{abs} for the absorption.

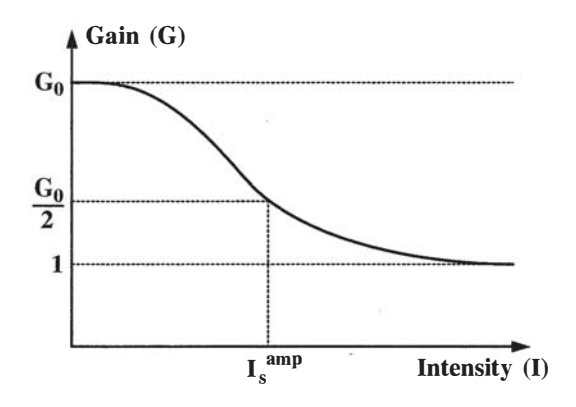


Figure 11.25: Gain through an amplifying medium as a function of the input intensity

Using these parameters, we can describe how a pulse arises in a passively mode-locked laser comprising the elements shown in Fig. 11.23. At the instant t=0 the pump beam is applied to the amplifying medium. The power inside the cavity is initially zero and the unsaturated gain G_0 is greater than the sum of all the cavity losses. An oscillation arises inside the cavity with a characteristic electromagnetic field showing very strong fluctuations at low power. As the power increases, the strongest intensity maxima start to saturate the absorbing medium. These stronger maxima thus suffer smaller losses than the lesser intensity maxima of the fluctuating field. Therefore the strongest maximum will eliminate the others in the competition for gain which occurs

inside the amplifying medium, since it will grow faster and will stifle all competing processes. If the conditions are favorable, it will end up by being the only intensity maximum in the cavity and will contain all the energy of the wave.

Let us now follow the pulse along its round trip through the cavity. Let us start at the point where the pulse which will eventually take over is already formed, but has not reached its final

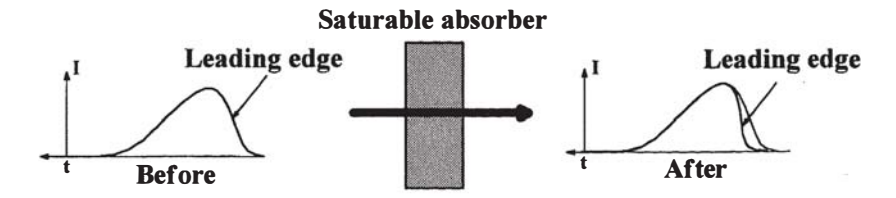


Figure 11.26: Illustration of pulse shape modification after crossing a saturable absorber

shape nor its final duration. As the pulse travels through the saturable absorber, the pulse front is strongly absorbed (Fig. 11.26), but if the maximum of the pulse saturates the absorber medium and if - as is the case in a dye laser or in a Ti:sapphire laser - the relaxation time of the medium is longer than the pulse duration, the tail of the pulse will benefit from the induced transparency of the medium and travel through it without being attenuated. When the pulse reaches the amplifying medium, the pulse front will come upon the unsaturated gain G_0 and will be strongly amplified while the tail of the pulse will feel a much weaker gain, which has just been saturated by the front of the pulse, and thus it will be much less amplified (Fig. 11.27). It is clear that after many back-and-forth trips, the resulting pulse will have narrowed and will have a very strong maximum, since the center of the initially broad pulse is not affected by the absorber but is amplified by the amplifying medium. This process is illustrated in Fig. 11.28. The fact that the saturation dynamics of the absorber are more rapid than those of the amplifying medium explains why only the center of the pulse is amplified, the wings, on the contrary, being attenuated.

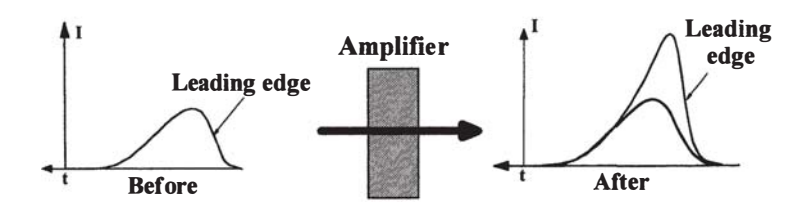


Figure 11.27: Illustration of pulse shape modification after crossing an amplifying medium

The pulse reaches its final shape when it becomes self-consistent in the cavity, that is, when the system reaches a steady state. For the pulse to be self-consistent, it must keep the same shape after a round trip through the cavity. However, the previous paragraph suggests that the pulse should grow ever narrower upon traveling constantly back and forth. Of course, if applied with sufficient care, the laws of physics will show that there is a limit to this process. As said earlier, the pulse duration under perfect mode-locked conditions is inversely proportional to the spectral width of the amplitude distribution. Therefore, each element of the cavity which tends to limit the width of the oscillation band will tend to lengthen the pulse duration. The element which is determining from this point of view may be an external optical element such as a prism, a grating or a Lyot filter. The amplifying medium itself may also be the determining element.

This broadening effect is best explained in the frequency domain. Just before entering the filtering element, the pulse has a spectral distribution with certain amplitudes. The transmission filter, which is frequency dependent, changes the distribution by decreasing the amplitudes of the wing frequencies while leaving the central frequencies unchanged. The narrowing of the spectrum explains the lengthening of the pulse duration as it passes through the filtering element. Similarly, each dispersive element of the cavity will also affect the pulse duration by time-delaying the various frequency components of the spectral distribution by different amounts. The pulse reaches steady state when the narrowing effect due to the saturation properties of the absorber and of

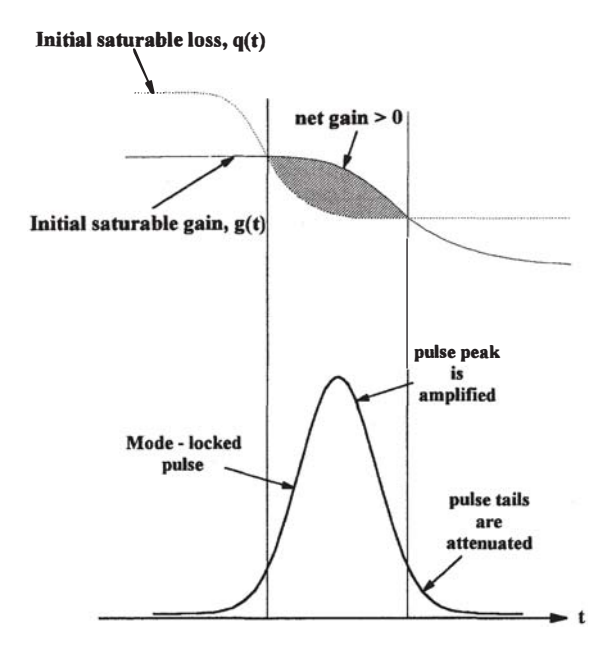


Figure 11.28: Illustration of the pulse-shortening process by simultaneous action of a saturable absorber and amplifying medium, due to saturation effects of the absorption and of the gain

the amplifying medium is exactly compensated by the broadening effects of the various elements in the cavity, of which the main two have been described above. In fact, the actual study of the propagation of the pulse through the various elements of the cavity is extremely complex, especially if one remembers that amplifying media and absorbers are nonlinear media. To tackle the problem in a reasonably realistic way, one should take into account, among other things, the variation of the refractive index with intensity inside these media. This variation results in a self-modulation of the phase of the pulse.

11.6 Kerr Lens Mode Locking ⁹

Self-Locking of the Modes

We have seen that the nonlinear properties of the amplifying medium are always very important for the locking process, whether the locking method is active or passive. In some types of lasers, these properties are so fundamental that the modes may lock, partially or totally, without any need for an external modulation (active locking), or for a saturable absorbing medium (passive locking). This situation is called self-locking of the modes. For such a situation to arise, the amplifying medium must induce a narrowing of the pulse at each of its round trips through the cavity. The dynamics which were described for the passive locking method show that saturation of the gain is not sufficient. There needs to be an associated effect which favors strong intensity maxima at the expense of weak ones. This effect is provided by the saturable absorber in the passive mode-locking method. We shall now describe a specific self-locking situation in which the amplifying medium decreases the losses of the stronger intensity peaks of the cavity by modifying the transverse structure of the laser wave selectively with respect to intensity. This situation exists in the Ti:sapphire laser, explaining why the interest in self-locking of modes suddenly flared up recently.

Historically speaking, the self-locking of modes was first observed accidentally in a laser whose

⁹Chapter 3 (Page 77 - 81) - Femtosecond laser pulses : principles and experiments -Rulliere, Claude - New York : Springer, 2005

 $^{^{10}}$ Source: Recent developments in compact ultrafast lasers, Ursula Keller, insight review articles, NATURE, VOL 424, 14 AUGUST 2003

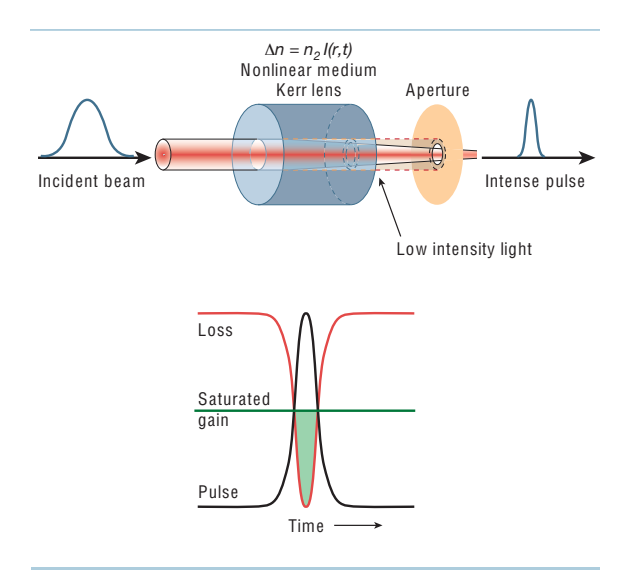


Figure 11.29: Kerr lens mode locking is obtained through a Kerr lens at an intracavity focus in the gain medium or in another material, where the refractive index increases with intensity $\Delta n = n_2 I(r,t)$, where n_2 is the nonlinear refractive index and I(r,t) the radial and time-dependent intensity of a short-pulsed laser beam. In combination with a hard aperture inside the cavity, the cavity design is made such that the Kerr lens reduces the laser mode area for high intensities at the aperture and therefore forms an effective fast saturable absorber. In most cases, however, soft-aperture KLM is used, where the reduced mode area in the gain medium improves for a short time the overlap with the (strongly focused) pump beam and therefore the effective gain. A significant change in mode size is only achieved by operating the laser cavity near one of the stability limits of the cavity. 10

amplifying medium consisted of a Ti:sapphire crystal pumped by an Ar⁺ laser, which, in principle, operated in a continuous regime, in a cavity without a saturable absorber. Scottish scientists then noticed that the laser went into a pulsed regime when they jerked the table on which the laser was mounted. The pulsed regime consisted of very short pulses, and once initiated, maintained itself. It was first called "magic mode locking", but it stayed magic only for a few months, an explanation having been found meanwhile. In fact, it was a case of self-locking by a Kerr lens effect [Kerr lens mode-locking (KLM)], a self-locking process which clearly reveals that the following conditions are needed for this kind of behavior to appear:

- The pulsed regime must somehow be favored over the continuous regime.
- The overall system must possess the property of shortening the pulses.
- Some mechanism must initiate the self-locking process.

Figure 11.30 shows the classical configuration of a self-mode-locked Ti:sapphire laser. The Ti:Al₂O₃ crystal is pumped by the output of a continuous Ar⁺ laser through M₂, a dichroic mirror which is transparent at 0.5 μ m and which reflects at the emission wavelengths of Ti:sapphire around 0.8 μ m. The birefringent filter (B.R.F.) determines the central wavelength of the oscillation. The two prisms P₁ and P₂ compensate for the dispersion of the group velocity inside the cavity, as was explained above. The mode-locking process arises exclusively from the amplifying medium and an associated pinhole with adjustable diameter. This process results from the Kerr effect and can be summarized in the following way.

The fact that the amplifying medium is nonlinear implies that its refractive index is a function of the intensity (Kerr effect): $n = n_0 + n_2 I$. The Gaussian wave therefore does not feel a homogeneous refractive index as it passes through the medium. If n_2 , the nonlinear coefficient of the refractive index, is positive, the refraction is stronger on the axis of the beam than away from it. So the amplifying medium behaves like a converging lens and focuses the beam just like a lens (Kerr

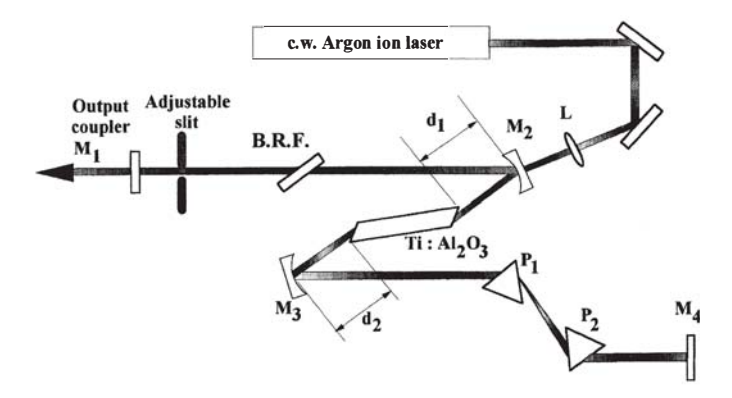


Figure 11.30: Typical cavity design of a self-mode-locked Ti:sapphire laser using the KLM (Kerr lens mode-locking) process (see text)

lens). We are speaking of the phenomenon of self-focusing, which has been known for a long time in nonlinear optics. However, self-focusing is proportionally more important for strong intensities. This means that the strong intensity maxima of the laser cavity will be much more strongly focused than the weaker ones, for which focusing will be negligible (Fig. 11.31).

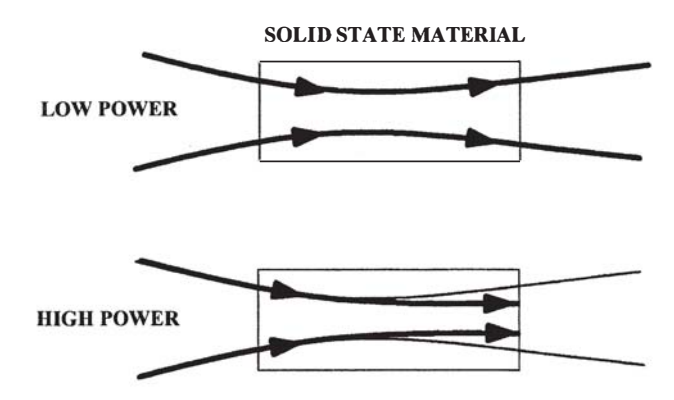


Figure 11.31: Illustration of the self-focusing effect by the optical Kerr effect on the beam waist of a laser beam at high and low intensity

These strong intensity maxima, whose transverse structures have now been reduced in size, are usually less subject to losses in the cavity than the weaker intensities, which occupy a large volume, so they are enhanced. Clearly, the intensity-differentiated self-focusing associated with the natural cavity losses plays a part similar to that of the saturable absorber in the passive mode-locking method, and, indeed, self-mode-locking of the modes arises. A slit can be placed inside the cavity to help the self-locking process since it increases the difference between the losses undergone by the weak intensities and those undergone by the intensity maxima. The exact position, diameter, and shape of the slit must be calculated so that it lets through most of the power of the stronger intensity maxima while it stops the greater part of the weaker intensities. Figure 11.32 illustrates the passage from a continuous regime (with open slit) to a mode-locked regime. The experimental data of Fig. 11.32 clearly show the broadening of the spectrum and its transformation into a spectrum corresponding to a correctly mode-locked regime for a slit width of 0.47 mm. It should be noted that the amplifying medium must be relatively thick to observe a strong lens effect. This explains why the lens effect, which is so important in the Ti:sapphire laser, is negligible in dye lasers.

The laser illustrated in Fig. 11.30 has the drawback that it does not go into the pulsed regime spontaneously. As long as no important intensity fluctuations arise to create sufficiently strong Kerr lens effects, the continuous regime prevails over the pulsed regime, as shown in Fig. 11.32. To start the pulsed process, one can insert a rapidly rotating optical slide so as to create a changing

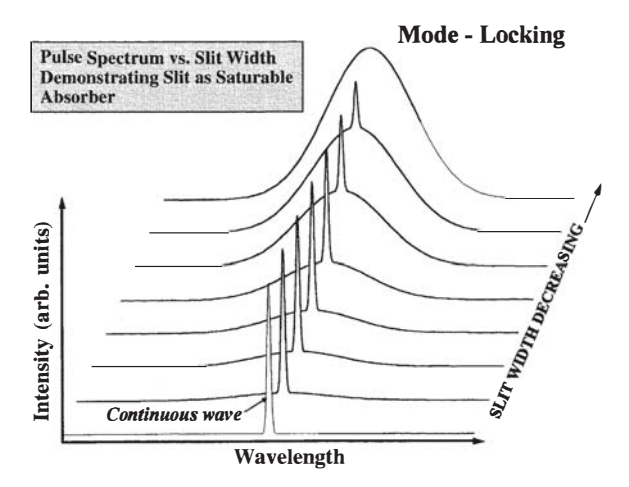


Figure 11.32: Spectral distribution of laser output for different widths of the slit inserted in the cavity, which controls the mode-locking by the optical Kerr effect

optical path, or one can simply give a quick jolt to one of the mirrors of the cavity to create an intensity pulse which triggers off the process.

We see therefore that in a Kerr-lens mode-locked (KLM) laser, the discrimination between a continuous regime and a pulsed regime is due to the self-focusing in the amplifying medium, and this discrimination becomes effective after a rapid transient change in the optical length of the cavity. We still have to explain how the pulses shorten and stabilize their duration by following their journey back and forth through the cavity in the proper self-locking conditions defined above. In fact, on top of its influence on the spatial evolution of the wavefront (self-focusing), the change of refractive index as a function of intensity in the amplifying medium also has very important consequences for the time structure of the laser wave. Indeed, the intensity I(t) being a rapidly varying function of time, the change of refractive index as a function of the intensity, following the equation $n = n_0 + n_2 I(t)$, implies a rapid change of the phase of the wave as a function of time. This self-modulation of the phase broadens the spectrum of the wave and therefore shortens its duration. As was the case for the passive mode-locking method, an equilibrium is reached between this process of pulse shortening and the dispersion of the group velocity, which tends to lengthen the pulse. The compensation between the self-modulation of the phase and the dispersion of the group velocity gives rise to a pulse which travels back and forth in the cavity while keeping its shape. This pulse is called a quasi-soliton. Here again, it is essential to be able to keep control of the group velocity inside the cavity, which is the reason for the two prisms in the system shown in Fig. 11.30.

This kind of mode-locking leads to excellent results for the pulse duration as well as for its stability. In Fig. 11.33 we show the autocorrelation trace and the spectrum of the pulse a few tens of femtoseconds wide obtained with the laser shown in Fig. 11.33. The ease with which these systems are made to work, their great reliability and the great stability from pulse to pulse place them among to day's most popular mode-locked systems. At present, they are chosen routinely each time a good-quality femtosecond oscillator is required.

11.7 Propagation of a Pulse in a Transparent Media ¹¹

What happens to a short optical pulse propagating in a transparent medium? Because of its wide spectral width and because of group velocity dispersion in transparent media, it undergoes a phase distortion inducing an increase of its duration. This happens with any optical element and needs to be properly corrected for in the course of experiments.

¹¹Chapter 2 (Page 32 - 38) - Femtosecond laser pulses: principles and experiments -Rulliere, Claude - New York: Springer, 2005

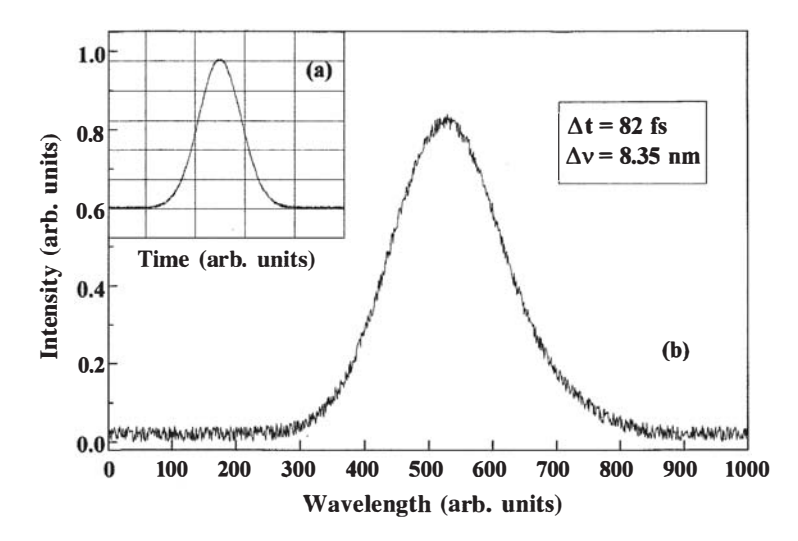


Figure 11.33: (a) Autocorrelation trace (b) and spectrum of the pulse a few hundreds of femtoseconds wide obtained with the laser shown in Fig. 11.30 after starting the mode-locking process

The frequency Fourier transform of a Gaussian pulse has already been given as

$$E_0(\omega) = e^{\frac{-(\omega - \omega_0)^2}{4\Gamma}} \tag{11.7.1}$$

After the pulse has propagated a distance x, its spectrum is modified to

$$E(\omega, x) = E_0(\omega)e^{\pm ik(\omega)x}, \qquad k(\omega) = n\omega/c$$
 (11.7.2)

where $k(\omega)$ is now a frequency-dependent propagation factor. In order to allow for a partial analytical calculation of the propagation effects, the propagation factor is rewritten using a Taylor expansion as a function of the angular frequency, assuming that $\Delta\omega \ll \omega_0$ (this condition is only weakly true for the shortest pulses). Applying the Taylor expansion

$$k(\omega) = k(\omega_0) + k'(\omega - \omega_0) + \frac{1}{2}k''(\omega - \omega_2)^2 + \dots$$
 (11.7.3)

where

$$k' = \left(\frac{dk(\omega)}{d\omega}\right)_{\omega_0} \tag{11.7.4}$$

and

$$k'' = \left(\frac{d^2k(\omega)}{d\omega^2}\right)_{\omega_0} \tag{11.7.5}$$

to (11.7.2), the pulse spectrum becomes

$$E(\omega, x) = \exp\left[-ik(\omega_0)x - ik'x(\omega - \omega_0) - \left(\frac{1}{4\Gamma} + \frac{i}{2}k''\right)(\omega - \omega_0)^2\right]$$
(11.7.6)

The time evolution of the electric field in the pulse is then derived from the calculation of the inverse Fourier transform of (11.7.6),

$$\epsilon(t,x) = -\frac{1}{2\pi} \int_{-\infty}^{+\infty} E(\omega,x)e^{i\omega t} d\omega$$
 (11.7.7)

so that

$$\epsilon(t,x) = \sqrt{\frac{\Gamma(x)}{\pi}} \exp\left[i\omega_0 \left(t - \frac{x}{v_\phi(\omega_0)}\right)\right] \times \exp\left[-\Gamma(x) \left(t - \frac{x}{v_g(\omega_0)}\right)^2\right]$$
(11.7.8)

where

$$v_{\phi}(\omega_0) = \left(\frac{\omega}{k}\right)_{\omega_0}, \quad v_g(\omega_0) = \left(\frac{d\omega}{dk}\right)_{\omega_0}, \quad \frac{1}{\Gamma(x)} = \frac{1}{\Gamma} + 2ik''x$$
 (11.7.9)

In the first exponential term of (11.7.8), it can be observed that the phase of the central frequency ω_0 is delayed by an amount x/v_{ϕ} after propagation over a distance x. Because the phase is not a measurable quantity, this effect has no observable consequence. The phase velocity $v_{\phi}(\omega)$ measures the propagation speed of the plane-wave components of the pulse in the medium. These plane waves do not carry any information, because of their infinite duration.

The second term in (11.7.8) shows that, after propagation over a distance x, the pulse keeps a Gaussian envelope. This envelope is delayed by an amount $x/v_g, v_g$ being the group velocity. Figure 11.34 shows schematically the relationship between the phase and the group velocities.

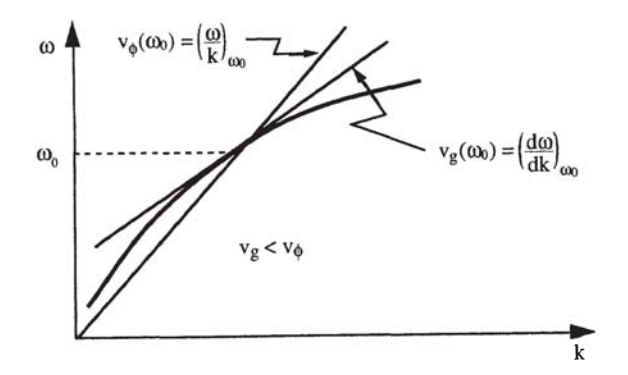


Figure 11.34: Schematic relationship between the phase and group velocities in an ordinary transparent medium. Note that this relationship does not depend on the sign of the curvature of the dispersion curve $\omega(k)$

The phase velocity $v_{\phi}(\omega_0)=(\omega_0/k)$ is the slope of a straight line starting at the origin and crossing the dispersion curve $\omega(k)$ where the angular frequency equals ω_0 . The group velocity $v_g(\omega_0)=(d\omega/dk)_{\omega_0}$ is the slope of the line tangential to the dispersion curve at the same point. In ordinary matter, $v_g< v_{\phi}$.

From the expression for the propagation factor $k=2\pi/\lambda$ and the expression for the wavelength in a medium $\lambda=2\pi c/\omega n(\omega), n(\omega)$ being the index of refraction, one gets

$$v_{\phi} = \frac{c}{n(\omega)} \tag{11.7.10}$$

$$v_g = \frac{d\omega}{dk} = \frac{1}{dk/d\omega}, \quad \frac{dk}{d\omega} = \frac{1}{c} \left(n(\omega) + \omega \frac{dn(\omega)}{d\omega} \right)$$
 (11.7.11)

$$v_g \approx v_\phi \left(1 - \frac{\omega}{n(\omega)} \frac{dn(\omega)}{d\omega}\right)$$
 (11.7.12)

The second term in (11.7.8) also shows that the pulse envelope is distorted during its propagation because its form factor $\Gamma(x)$, defined as

$$\boxed{\frac{1}{\Gamma(x)} = \frac{1}{\Gamma} + 2ik''x} \tag{11.7.13}$$

depends on the angular frequency ω through $k''(\omega)$,

$$k'' = \left(\frac{d^2k}{d\omega^2}\right)_{\omega_0} = \frac{d}{d\omega} \left(\frac{1}{v_g(\omega)}\right)$$
 (11.7.14)

This term is called the "group velocity dispersion".

Rewriting $\Gamma(x)$ as

$$\Gamma(x) = \frac{\Gamma}{1 + \xi^2 x^2} - i \frac{\xi x}{1 + \xi^2 x^2}, \quad \xi = 2\Gamma k''$$
 (11.7.15)

and substituting (11.7.15) into the second term of the right-hand side of (11.7.8) yields the following expression:

$$\exp\left[-\frac{\Gamma}{1+\xi^2 x^2} \left(t - \frac{x}{v_g}\right)^2 + i \frac{\xi x}{1+\xi^2 x^2} \left(t - \frac{x}{v_g}\right)^2\right]$$
 (11.7.16)

The real part of (11.7.16) is still a delayed Gaussian function. Its form factor

$$\frac{\Gamma}{1+\xi^2 x^2} \tag{11.7.17}$$

is always smaller than the original one Γ , which means that the pulse undergoes a duration broadening. Figure 11.35 shows a sketch of the pulse envelope broadening during its propagation through a transparent medium. The phase, i.e. imaginary part in (11.7.16), contains a quadratic time term

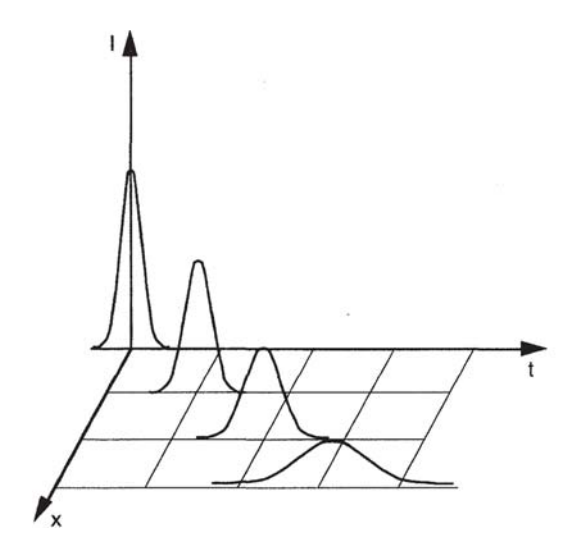


Figure 11.35: Numerical calculation of the intensity envelope of a pulse propagating along x, in a lossless, transparent medium. The pulse broadens with time but, from energy conservation, its time-integrated intensity remains constant

and we have already seen that this creates a linear frequency chirp in the pulse

In summary, the propagation of a short optical pulse through a transparent medium results in a delay of the pulse, a duration broadening and a frequency chirp.

Dispersion Parameter of a Transparent Medium.

The dispersion of an index of refraction is usually tabulated as a function of the wavelength of light in vacuum. We therefore need to recalculate the dispersion as a function of the wavelength. From (11.7.14) we obtain

$$k'' = -\frac{\lambda^2}{2\pi c}D, \qquad D = \frac{1}{L}\frac{dt_g}{d\lambda}$$
 (11.7.18)

with t_g being the group delay induced by propagation over length L. D is called the dispersion parameter. The group delay t_g is calculated using (11.7.12) for the group velocity and the simple definition $t_g = L/v_g$, which leads to

$$k'' = \frac{\lambda^3}{2\pi c^2} \frac{d^2 n}{d\lambda^2} \tag{11.7.19}$$

The sign of k'' depends on the curvature of the dispersion of the index $d^2n/d\lambda^2$.

A one-resonance Drude model is the simplest way to describe the electronic properties of matter. In this very simple model the variation of the index of refraction in the vicinity of the resonance looks as shown in Fig. 11.36.

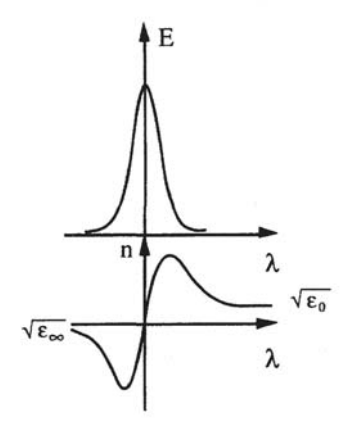


Figure 11.36: (Top) sketch of an electronic resonance, from which the index of refraction (bottom) can be calculated

For wavelengths larger than the resonance wavelength the curvature of the index dispersion curve is positive (upward concavity) and the group velocity dispersion is positive (k'' > 0). This situation is the most usual one, encountered in ordinary optical glasses in the visible range. The index of refraction diminishes as the wavelength increases, which in turn implies an increase of the group velocity: in a light pulse propagating through a transparent medium, the instantaneous frequency varies from its lowest in the leading edge to its highest in the trailing edge. Notice from (11.7.19) that a positive group velocity dispersion corresponds to a negative dispersion parameter D.

For wavelengths below the electronic resonance the situation is reversed and the group velocity dispersion is negative. This situation can be found in silica optical fibers, where a single resonance takes place, due to OH vibrations. For wavelengths around 1.55 μ m, the group velocity is negative, allowing the propagation of optical solitons.

Time Compression with a Pair of Gratings.

In order to correct for group-velocity-dispersion distortions, several optical devices have been designed that have an overall negative group velocity dispersion. As an example we consider a pair of transmission gratings R_1 and R_2 . These gratings have a groove spacing d and their separation is l (Fig. 11.37).

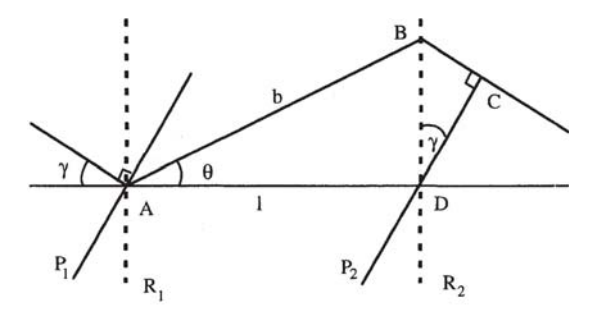


Figure 11.37: Optical path through a pair of transmission gratings

A light ray, with wavelength λ , impinges on grating R_1 with an angle of incidence γ and is scattered with an angle θ . The gratings are set in such a way that their wavelength dispersions

are reversed, which implies that the exiting ray at point B is parallel to the incident ray. P_1 and P_2 are wave planes at the entrance A and exit B of the system. P_2 crosses the emerging ray at point C. Between points A and B the light travels a distance $b = l/\cos\theta$. The diffraction due to a grating can be written as

$$d(\sin\gamma + \sin\theta) = \lambda \tag{11.7.20}$$

In order to calculate the dispersion from (11.7.19), the group delay experienced by the light must first be evaluated. In this specific case, where propagation takes place only in air, the group delay is simply equal to the travel time of light along ABC,

$$t = L/c = (AB+BC)/c,$$
 $BC=DB \sin \gamma = b \sin \theta \sin \gamma$ (11.7.21)

$$t = -\frac{b}{c}(1 + \sin\theta\sin\gamma) \tag{11.7.22}$$

and the dispersion parameter is expressed as

$$D = \frac{1}{b} \frac{dt}{d\lambda} \tag{11.7.23}$$

which from (11.7.20), applying a small-angle approximation, yields

$$D = \frac{\lambda}{cd^2} \left[1 - \left(\frac{\lambda}{d} - \sin \gamma \right)^2 \right]^{-1} \tag{11.7.24}$$

$$k'' = -\frac{\lambda^3}{2\pi c^2 d^2} \left[1 - \left(\frac{\lambda}{d} - \sin \gamma \right)^2 \right]^{-1}$$
 (11.7.25)

This expression demonstrates the possibility of selecting a set of parameters in such a way as to design a pair of gratings producing a positive or a negative group velocity dispersion. Therefore optical devices can be built that compensate a positive group velocity dispersion suffered by optical pulses traveling through a transparent material. Optical compressors have been a key to the development of various fields in which short optical pulses have been used as a primary tool. Figure 11.38 shows a typical arrangement for a reflective pulse compressor.

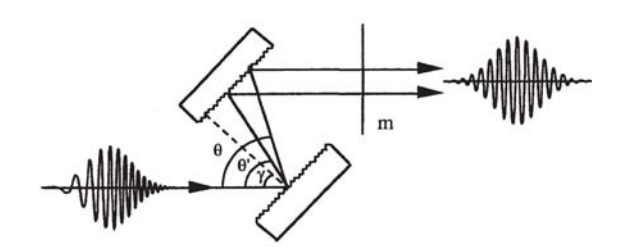


Figure 11.38: Grating optical compressor. Two gratings are set in a subtractive diffraction geometry. Red components of a light pulse have a longer optical path than blue ones. The various components of a positively dispersed pulse can therefore be reset in phase.